

# Super-resolution imaging using a three-dimensional metamaterials nanolens

B. D. F. Casse,<sup>a)</sup> W. T. Lu, Y. J. Huang, E. Gultepe, L. Menon, and S. Sridhar<sup>a)</sup>

*Department of Physics and Electronic Materials Research Institute, Northeastern University, Boston, Massachusetts 02115-5000, USA*

(Received 14 November 2009; accepted 21 December 2009; published online 14 January 2010)

Super-resolution imaging beyond Abbe's diffraction limit can be achieved by utilizing an optical medium or "metamaterial" that can either amplify or transport the decaying near-field evanescent waves that carry subwavelength features of objects. Earlier approaches at optical frequencies mostly utilized the amplification of evanescent waves in thin metallic films or metal-dielectric multilayers, but were restricted to very small thicknesses ( $\ll \lambda$ , wavelength) and accordingly short object-image distances, due to losses in the material. Here, we present an experimental demonstration of super-resolution imaging by a low-loss three-dimensional metamaterial nanolens consisting of aligned gold nanowires embedded in a porous alumina matrix. This composite medium possesses strongly anisotropic optical properties with negative permittivity in the nanowire axis direction, which enables the transport of both far-field and near-field components with low-loss over significant distances ( $>6\lambda$ ), and over a broad spectral range. We demonstrate the imaging of large objects, having subwavelength features, with a resolution of at least  $\lambda/4$  at near-infrared wavelengths. The results are in good agreement with a theoretical model of wave propagation in anisotropic media. © 2010 American Institute of Physics. [doi:10.1063/1.3291677]

Image formation by a lens is subject to a fundamental limit of resolution of any optical system known as "Abbe's diffraction limit"—features of an object smaller than  $\lambda/2$  ( $\lambda$ , wavelength) cannot be imaged by conventional optics.<sup>1</sup> Abbe's diffraction limit arises because evanescent waves which carry sub- $\lambda$  information decay exponentially, leaving only the propagating waves that carry low frequency spatial components (coarser details) to be collected at the image plane. Almost ten years ago, Pendry discussed the possibility of restoring these evanescent waves using the amplifying property of a slab of "metamaterial" which has a negative refractive index.<sup>2</sup> The mechanism behind amplification of the evanescent waves in this perfect lens is the resonant excitation of surface waves supported at the interfaces of the metamaterials slab. Several approaches, based on Pendry's archetype, to creating optical components with negative-index metamaterials for super-resolution imaging have been investigated.<sup>3–6</sup> However, at optical frequencies, negative-index metamaterials<sup>7–9</sup> constructed from realistic materials (in particular resonance-based metallic elements) are intrinsically associated with loss (imaginary part of permittivity  $\epsilon$  or permeability  $\mu$ ), which in turn hinders the resolution of the optical components.<sup>10</sup> Besides the severe limitations of material loss, the predominant shortcomings of these super-resolution lenses are the narrow spectral bandwidth at which they operate, the small thickness of the lens (poor man's lens<sup>11,12</sup>), image distortions (photonic crystals<sup>13</sup>), limited imaging area (hyperlens<sup>14</sup>), lack of support for propagating waves (poor man's lens/subwavelength plates<sup>15</sup>), and the fact that information needs to be collected from multiple measurements (far-field grating superlens<sup>16</sup>).

An innovative approach, which makes use of arrays of high aspect ratio metallic wires,<sup>17,18</sup> has been theoretically suggested to mitigate the aforementioned drawbacks. The

underlying mechanism for restoring evanescent waves in such metallic wires medium, is not based on resonances of materials parameters (i.e., there is no amplification machinery from excitation of surface waves at interfaces), but is rather based on the transport of evanescent waves when the medium exhibits a relatively flat equifrequency dispersion characteristics. In this case the medium can reconstruct sub-wavelength details of an object not only with low-loss but also over a broad frequency range. Specifically, it was proposed that aligned metallic nanowires embedded in dielectric matrices possess strongly anisotropic optical properties with negative permittivity  $\text{Re } \epsilon_z < 0$  along the nanowire axis and positive permittivity  $\text{Re } \epsilon_{x,y} > 0$  in the transverse plane, that can be used to achieve broadband all-angle negative refraction and superlens imaging.<sup>19</sup> This medium is an example of so-called indefinite media.<sup>20</sup> To date, sub- $\lambda$  imaging experiments, by means of such wire array media, have been restricted to microwave frequencies,<sup>21,22</sup> mainly due to the challenge in manufacturing extreme high aspect ratio metallic wires at a nanoscale level.

In this letter, we report super-resolution imaging by a low-loss three-dimensional (3D) metamaterial nanolens, with a resolution of at least  $\lambda/4$  at near-infrared wavelengths and over a significant distance (or thickness) of  $>6\lambda$  (Fig. 1). This metamaterials nanolens consists of bulk high aspect ratio aligned gold nanowires embedded in a porous alumina host matrix of thickness  $10 \mu\text{m}$ . The composite medium is fabricated by a combination of bottom-up self assembly and electrochemical process.<sup>23</sup> Earlier optical measurements have shown that for long wavelengths, in the infrared,<sup>23</sup> the material has strongly anisotropic optical properties with negative permittivity  $\text{Re } \epsilon_z < 0$  along the nanowire ( $z$ ) axis and positive permittivity  $\text{Re } \epsilon_{x,y} > 0$  in the transverse ( $x, y$ ) plane (Fig. 2). Optical negative refraction in these bulk metamaterials of metallic nanowires has been recently reported.<sup>24</sup> The lens can be manufactured on a large scale, and a representative sample 3/4 of the size of a U.S. penny is shown in Fig.

<sup>a)</sup>Authors to whom correspondence should be addressed. Electronic addresses: d.casse@neu.edu and s.sridhar@neu.edu.

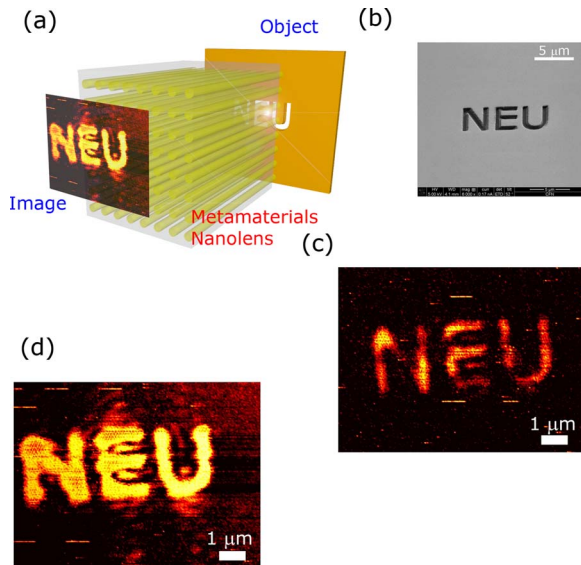


FIG. 1. (Color online) (a) Imaging with subwavelength resolution by the metamaterial nanolens at 1550 nm. The nanolens consists of high aspect ratio metallic nanowires which are embedded in a host dielectric medium. This bulk metamaterial transports subwavelength details of an object at a significant distance of more than six times the wavelength ( $\lambda$ ). (b) Scanning electron microscope (SEM) image of the “NEU” letters (acronym for Northeastern University) milled in 100 nm thick gold metallic film. The letters have 600 nm wide arms ( $0.4\lambda$ ). (c) Near-field scanning optical microscope (NSOM) scan of the source object in the near-field at 1550 nm wavelength. (d) NSOM scan of the corresponding image by the metamaterial nanolens above the nanolens surface.

2(a). A 3D oblique view illustration of a section of the nanolens, portraying the metamaterial nanostructural design is shown in Fig. 2(b). In the scanning electron microscope (SEM) picture representing the top-view of the nanolens [shown in Fig. 2(c)], the tips of the nanowires can be seen on the surface. An SEM picture of a cross-section of the 10  $\mu\text{m}$  thick porous alumina template is shown in Fig. 2(d). The

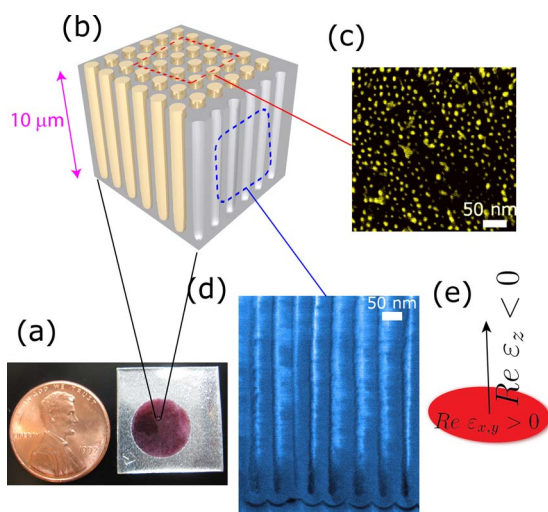


FIG. 2. (Color online) (a) Bulk metamaterial (pink circle) manufactured in large scale ( $>10$  mm in diameter or almost  $3/4$  the size of a U.S. penny). (b) 3D illustration of the nanoscale architecture of the nanolens. (c) Top view: SEM image showing the tips of the gold nanowires. The metamaterial nanolens consists of aligned gold nanowires, with 12 nm diameters and lattice spacing of 25 nm, embedded in porous alumina template matrix. (d) Side view: SEM image of the cross-section of the 10  $\mu\text{m}$  thick nanoporous alumina template without the gold nanowires. (e) Anisotropic optical property of the metamaterial: Negative permittivity in the nanowire axis  $z$  direction ( $\text{Re } \epsilon_z < 0$ ) and positive permittivity in the  $x$ - $y$  plane ( $\text{Re } \epsilon_{x,y} > 0$ ).

nanopores are 12 nm in diameter and have an average spacing of 25 nm.

The schematic of imaging with the metamaterials nanolens is depicted in Fig. 1(a). In our experiment, the object (void pattern) with subwavelength features is illuminated with a continuous wave (cw) laser at 1550 nm. The void pattern was milled by focused ion beam lithography on a 100 nm thick metallic film deposited on 0.1 mm thick glass substrate. After passing through the nanolens, the transmitted beam is then mapped with a near-field scanning optical microscope (NSOM) probe above the nanolens surface. The representative object imaged consists of the letters “NEU” (acronym for Northeastern University) with 600 nm wide ( $0.4\lambda$ ) arms, as shown in the SEM picture in Fig. 1(b). The NSOM scan of this source object illuminated by the laser light is shown in Fig. 1(c). NSOM scans were carried out at the far end of the metamaterial nanolens (image plane). As illustrated in Fig. 1(d), the subwavelength letters were clearly resolved with very low distortions.

For a complete set of control experiments, we have also attempted to image the “NEU” letters with (a) porous alumina template without the gold nanowires (essentially a pure dielectric) and (b) 10  $\mu\text{m}$  above the surface of the object in air without the alumina template (not shown). For both cases, the images were almost unrecognizable in the far-field and super-resolution imaging was not achieved, demonstrating that the composite metamaterial behaves as a super-resolution medium.

To demonstrate the broadband aspect of the lens, imaging experiments were performed within the tunable wavelength range of our near-infrared laser (i.e., 1510–1580 nm) (not shown). No significant distortions were observed when the wavelength was varied from 1510 to 1580 nm, indicating that some degree of broadband imaging ( $\sim 5\%$ ) is also realizable with this nanolens. Theoretically, the nanolens will also operate at longer wavelengths, up to 21 microns.<sup>19</sup>

In order to assess the resolving capability (or resolution) of the lens, imaging of a subwavelength two-slit object was carried out. The two-slit object in this case is composed of two 600 nm ( $\sim 0.4\lambda$ ) slits spaced 400 nm ( $0.26\lambda$ ) apart [inset of Fig. 3(c)]. Figures 3(a) and 3(b) show the NSOM map of the source object and image, respectively. Experimentally, we find that the slits can be clearly resolved by the bulk nanolens even though their critical dimensions are much smaller than the wavelength [Fig. 3(b)]. The smallest length scale, i.e., the edge-to-edge distance of 400 nm, is clearly distinguished indicating that the lens has a resolution capability of at least  $\lambda/4$  for the near infrared spectral range [Fig. 3(c)]. The curve for a conventional optical microscope is also shown, demonstrating that the two individual slits cannot be resolved by a diffraction-limited optical system.

The above experiments clearly establish that the metamaterial nanolens is a super-resolution medium which can transport, with low-loss, object details down to  $\lambda/4$  length scales, over large distances  $>6\lambda$ . Interestingly, attenuation by the metamaterial nanolens was recorded to be less than 1 dB/cm. Furthermore, the figure-of-merit (FOM) of the nanolens is given by  $\text{FOM} = -\text{Re}(n)/\text{Im}(n) \sim 12$ , which is  $4\times$  higher than the best fabricated metallic-based metamaterial at 1.5  $\mu\text{m}$ .<sup>25</sup>

The mechanism behind super-resolution reconstruction in this metamaterial is the transport of evanescent waves by

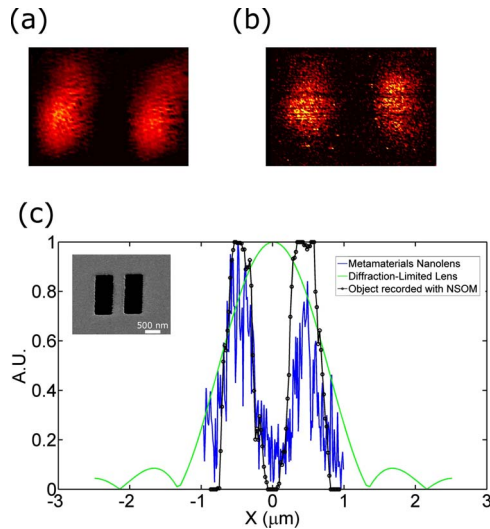


FIG. 3. (Color online) (a) NSOM scan of the object of the two-slit object illuminated at 1550 nm. (b) NSOM scan of the corresponding image by the nanolens of the two-slit object. (c) The intensity profile of the source object (M-shape) and image (M-shape, noisy) are plotted. The results indicate that the metamaterial nanolens has a resolution of at least  $\sim\lambda/4$  for the near-infrared spectral range. The intensity profile of the object as resolved by a diffraction-limited optical system is also plotted (Gaussian-like). The inset figure is an SEM image of the nanoslits.

guided modes through the engineered media. Imaging beyond Abbe's diffraction limit requires guided modes with flat isofrequency contours, where the longitudinal wave vector  $k_z$  ( $z$  is in the direction of the nanowires) is nearly independent of the transverse wave vector  $k_{x,y}$ . In arrays of metallic rods medium, in which the permittivity of nanowires is sufficiently negative ( $\text{Re } \epsilon_z < 0$ ), a quasi-TEM (transverse electromagnetic) nearly dispersionless mode capable of guiding evanescent waves is supported.<sup>18</sup> From both optical characterization<sup>23</sup> and analytical formula,<sup>19</sup> we have shown that the medium is strongly anisotropic ( $\text{Re } \epsilon_z < 0$  and  $\text{Re } \epsilon_{x,y} > 0$ ), corresponding to the situation where polarized electromagnetic modes can be excited. In this composite medium, the guided quasi-TEM mode does not effectively penetrate the metallic nanowires and thus most of the energy propagates in the host porous alumina dielectric medium in between the nanowires, so that the influence of the metallic wires losses are negligible. The mechanism is different from that in Ref. 26, where Ono *et al.* exploit the excitation and propagation of surface plasmon polaritons (SPPs) to achieve super-resolution imaging. Full-wave simulations and analytical derivations confirm that subwavelength details of an object can be transported along such wire arrays over long distances.<sup>18,27,28</sup>

The metamaterial nanolens has noteworthy advantages over other currently available metamaterials-based approaches to super-resolution imaging—earlier superlenses have been restricted to very small thicknesses ( $\ll\lambda$ ) (Refs. 11 and 12) or to two-dimensions<sup>13</sup> so that some degree of resonant enhancement of the evanescent waves can be obtained without being buried by material loss. In contrast to a grating far-field superlens, it needs only a single measurement to obtain a very large bandwidth in Fourier space to reconstruct super-resolution details of an object. And, in comparison to the poor man's superlens (thin film  $\sim 60$  nm of homogeneous negative permittivity  $\epsilon < 0$ ), the metamaterial nanolens support both propagating and evanescent waves required for

full imaging in a bulk medium ( $\sim 10 \mu\text{m}$ ). In addition, the poor man's superlens has a much narrower spectral bandwidth than the nanolens. Also, the metamaterial nanolens has theoretically no limitations on the imaging area (unlike the hyperlens) and the concepts described here are applicable over a broad spectral range, from far infrared up to UV frequencies, by suitable choice of material and filling factor, enabling broadband color imaging. The superior optical properties of these nanomaterials, coupled with large scale manufacturing, offer the potential for applications in transformation optics, nanolithography, and biomedical imaging.

The authors would like to thank M. G. Silveirinha, D. Heiman, J. Sokoloff, and F. Camino for useful discussions and comments. This work was financially supported by the Air Force Research Laboratories, Hanscom through Grant No. FA8718-06-C-0045 and NSF through Grant No. PHY-0457002. The work was also performed in part at the Kostas Center at Northeastern University and the Center for Nano-scale Systems, a member of NNIN, which is supported by the National Science Foundation under NSF Award No. ECS-0335765. Research carried out in part at the Center for Functional Nanomaterials, Brookhaven National Laboratory, which is supported by the U.S. Department of Energy, Office of Basic Energy Sciences, under Contract No. DE-AC02-98CH10886.

<sup>1</sup>E. Abbe, *Mikroskop. Anat.* **9**, 413 (1873).

<sup>2</sup>J. B. Pendry, *Phys. Rev. Lett.* **85**, 3966 (2000).

<sup>3</sup>X. Zhang and Z. Liu, *Nature Mater.* **7**, 435 (2008).

<sup>4</sup>J. Shin, J. T. Shen, and S. Fan, *Phys. Rev. Lett.* **102**, 093903 (2009).

<sup>5</sup>A. J. Hoffman, *Nature Mater.* **6**, 946 (2007).

<sup>6</sup>S. Kawata, Y. Inouye, and P. Verma, *Nat. Photonics* **3**, 388 (2009).

<sup>7</sup>B. D. F. Casse, H. O. Moser, M. Bahou, L. K. Jian, and P. D. Gu, 2006 IEEE Conference on Emerging Technologies - Nanoelectronics, pp. 328–331 (IEEE, 2006).

<sup>8</sup>V. M. Shalaev, *Nat. Photonics* **1**, 41 (2007).

<sup>9</sup>H. J. Lezec, J. A. Dionne, and H. A. Atwater, *Science* **316**, 430 (2007).

<sup>10</sup>V. A. Podolskiy and E. E. Narimanov, *Opt. Lett.* **30**, 75 (2005).

<sup>11</sup>N. Fang, H. Lee, C. Sun, and X. Zhang, *Science* **308**, 534 (2005).

<sup>12</sup>T. Taubner, D. Korobkin, Y. Urzhumov, G. Shvets, and R. Hillenbrand, *Science* **313**, 1595 (2006).

<sup>13</sup>B. D. F. Casse, W. T. Lu, R. K. Banyal, Y. J. Huang, S. Selvarasah, M. R. Dokmeci, C. H. Perry, and S. Sridhar, *Opt. Lett.* **34**, 1994 (2009).

<sup>14</sup>Z. Liu, H. Lee, Y. Xiong, C. Sun, and X. Zhang, *Science* **315**, 1686 (2007); I. I. Smolyaninov, Y.-J. Hung, and C. C. Davis, *ibid.* **315**, 1699 (2007).

<sup>15</sup>R. Merlin, *Science* **317**, 927 (2007).

<sup>16</sup>Z. Liu, S. Durant, H. Lee, Y. Pikus, N. Fang, Y. Xiong, C. Sun, and X. Zhang, *Nano Lett.* **7**, 403 (2007).

<sup>17</sup>R. Wangberg, J. Elser, E. E. Narimanov, and V. A. Podolskiy, *J. Opt. Soc. Am. B* **23**, 498 (2006).

<sup>18</sup>M. G. Silveirinha, P. A. Belov, and C. R. Simovski, *Phys. Rev. B* **75**, 035108 (2007).

<sup>19</sup>W. T. Lu and S. Sridhar, *Phys. Rev. B* **77**, 233101 (2008).

<sup>20</sup>D. R. Smith and D. Schurig, *Phys. Rev. Lett.* **90**, 077405 (2003).

<sup>21</sup>P. A. Belov, Y. Zhao, S. Tse, P. Ikonen, M. G. Silveirinha, C. R. Simovski, S. Tretyakov, Y. Hao, and C. Parini, *Phys. Rev. B* **77**, 193108 (2008).

<sup>22</sup>P. A. Belov, Y. Hao, and S. Sudhakaran, *Phys. Rev. B* **73**, 033108 (2006).

<sup>23</sup>L. Menon, W. T. Lu, A. L. Friedman, S. P. Bennett, D. Heiman, and S. Sridhar, *Appl. Phys. Lett.* **93**, 123117 (2008).

<sup>24</sup>J. Yao, Z. Liu, Y. Liu, Y. Wang, C. Sun, G. Bartal, A. M. Stacy, and X. Zhang, *Science* **321**, 930 (2008).

<sup>25</sup>G. Dolling, C. Enkrich, M. Wegener, C. M. Soukoulis, and S. Linden, *Opt. Lett.* **31**, 1800 (2006).

<sup>26</sup>A. Ono, J. I. Kato, and S. Kawata, *Phys. Rev. Lett.* **95**, 267407 (2005).

<sup>27</sup>M. G. Silveirinha, P. A. Belov, and C. R. Simovski, *Opt. Lett.* **33**, 1726 (2008).

<sup>28</sup>M. G. Silveirinha and N. Engheta, *Phys. Rev. Lett.* **102**, 103902 (2009).